Int. J. Heat Mass Transfer. Vol. 35, No. 6, pp. 1533–1544, 1992
Printed in Great Britain

0017-9310/92 $5.00+0.00

Thermal constriction resistance: effects of boundary conditions and contact geometries

KEK-KIONG TIO

Department of Applied Mechanics and Engineering Sciences, University of California at San Diego, La Jolla, CA 92093-0411, U.S.A.

and

S. S. SADHAL

Department of Mechanical Engineering, University of Southern California, Los Angeles, CA 90089-1453, U.S.A.

(*Received* 9 *July* 1990 *and in final form* 30 *April* 1991)

Abstract—The problem of steady-state thermal constriction resistance is modeled by means of various spatially periodic arrangements of circular disks (contact regions) on the surface of a semi-infinite solid. Three cases of disk boundary condition are considered: uniform flux, the 'equivalent isothermal flux', and the condition of isothermal disks. Analytical expressions for the resistance are derived as power series of $\kappa^{1/2}$, where κ is the fraction of the solid surface occupied by the disks. The behavior of the resistance is then studied as a function of disk boundary condition, spatial arrangement and concentration.

1. INTRODUCTION

It is well known that thermal contact resistance arises from the imperfect contact of two solid surfaces. The surface roughness brings about the situation in which the solids make contact with each other over discrete regions of the interface, leaving air gaps in the remainder. As a result, heat flowing across the interface is channelled through the contacting regions, the air gaps being practically impervious to heat flow. This causes a constriction in the heat flow near the interface and, therefore, there exists a resistance to the flow. This resistance is commonly called the thermal constriction resistance. The subject has been reviewed extensively in recent years, and excellent literature surveys are available [1–3].

For two semi-infinite solids in steady-state thermal contact, it is not difficult to show that the contacting regions have a uniform temperature. The problem thus reduces to that of one semi-infinite solid with isothermal discrete regions on the plane surface while the rest of the surface is considered insulated. The classical model is that of one circular contact on a semi-infinite solid, the solution to which is well known [4]. In the case of multiple contact regions, however, the problem becomes very complicated due to the multiply connected mixed Dirichlet and Neumann conditions at the solid surface. To overcome the difficulty of mixed boundary conditions, a number of investigators have replaced the isothermal condition with some prescribed heat fluxes. Beck [5], for example, treated the case of a square array of circular regions heated by a uniform flux. Another approach to the multiple contact problem is with the 'cylindrical cell' model. This model assumes that each contact region can be isolated with an adiabatic coaxial cylindrical surface within the solid. This method admits an axially symmetric solution, and has been quite popular [6–9].

In this paper, we consider the steady-state conduction in a semi-infinite solid with identical disks (circular contact regions) distributed periodically throughout the surface. Three cases of disk boundary condition will be considered, the rest of the solid surface being insulated: uniform flux; 'equivalent isothermal flux', which is the heat flux condition for *one* isothermal disk on a semi-infinite solid; and uniform temperature. Among these approximations of the physical problem, the case of isothermal contacts probably gives the best description. It is also the most difficult of these to solve. Of course, it is understood that there are some situations requiring the uniform flux condition at the contacting regions. Of main interest in this study will be the analytical derivation of the dimensionless resistance ψ defined by

$$\psi \equiv 4Rk\frac{\Delta T}{Q} \tag{1}$$

where R is the radius of the disks, k is the solid thermal conductivity, ΔT is the difference between the average temperature of the disks and the average temperature of the entire surface, and Q is the rate of heat flow into the solid through one disk. Then, the behavior of ψ will be studied as a function of disk boundary condition and disk spatial distribution. Three cases of disk arrangement will be considered: square array, hexagonal array, and triangular array.

NOMENCLATURE

b	distance between the reference disk and the neighboring disk under consideration
$h_i, h_{i,6}, H_i$	array sums, equations (21), (49), (24) and (25)
$H_i^*, H_{i,6}^*$	array sums, equations (23) and (48)
J_n	Bessel function of the first kind of order n
k	thermal conductivity
N	positive integer
P_n	Legendre polynomial of degree n
$\tilde{q}$	average surface heat flux
q_0	constant heat flux
q_E	equivalent isothermal flux
q_h, q_s	heat flux distributions over isothermal disks arranged in a hexagonal and a square array, respectively
Q	total rate of heat flow across one contact area
R	disk radius
$s_i, s_{i,4}, S_i$	array sums, equations (10), (47), (15) and (16)
$S_i^*, S_{i,4}^*$	array sums, equations (18) and (46)
t_i, T_i, T_i^*	array sums, equations (28) and (30)–(32)
T	temperature
$\bar{T}$	average temperature of contact regions
$\tilde{T}$	average temperature of solid surface
$\tilde{T}_A$	average temperature of the reference disk, A
T_{AB}	temperature rise at disk A due to disk B
$\bar{T}_{AB}$	T_{AB} averaged over disk A
ΔT	difference between average contact and average surface temperatures.

Greek symbols

δ	distance between a disk and its closest neighbor
Θ	equation (45)
κ	area fraction of contact regions
Λ	equation (60)
ψ	dimensionless constriction resistance
Ω	equation (58).

Subscripts

c	circular cell
h	hexagonal array
s	square array
t	triangular array.

Superscripts

eif	pertaining to disks with the equivalent isothermal flux
i	pertaining to isothermal disks
uf	pertaining to disks with a uniform flux.

Coordinate systems

(x, y, z)	rectangular coordinates
(ρ, ϕ, z)	cylindrical coordinates with the origin at the center of any one disk under consideration and ϕ measured from the x-axis (Figs. 2–4)
(r, ϕ, z)	cylindrical coordinates, origin at the center of the reference disk
(r, θ)	polar coordinates with θ measured from the line joining the reference disk and the neighboring disk under consideration (Fig. 1).

Situations involving spatially periodic contact areas arise in special cases such as those of machined surfaces. As discussed by Negus *et al.* [10], periodicity along with anisotropy arose in such situations. In general, the contact regions have random shape, size, and distribution. This fully random problem, however, is so difficult that an analytical solution does not appear to be feasible. For the less general problem of randomly placed circular contacts of the same size, an approximate solution can be worked out using Batchelor's [11] method. However, the solution is valid only for dilute contact concentrations. On the other hand, analytical solutions valid for a wide range of contact fractions can be obtained only when the contact regions are periodically distributed. In the interest of demonstrating the effects of disk arrangement for non-dilute cases, we have chosen the model of regularly arranged contact areas. As mentioned earlier, we consider three types of periodic array.

In view of the periodicity of the disk arrangement, we can reduce the problem to that of a circular contact region on top of a laterally insulated semi-infinite prism of square, hexagonal, or triangular cross-section. Negus and Yovanovich [12] treated the case of a circular contact on a square prism, and calculated the constriction resistance numerically. Analytical expressions for the constriction resistance were obtained by Sadhal [13] for an elliptical contact on a square prism by a double Fourier series eigenfunction expansion; these expressions, however, consisted of infinite double series of Bessel functions and converged very slowly for small contact sizes. In an aggregate study of various Fourier-type series solutions, Negus *et al.* [14] examined three types of contact geometries consisting of a circular contact on square and circular prisms and a square contact on a square prism, all with the uniform flux condition on the contact area. The Fourier method cannot be extended to cover hexagonal or triangular prisms since it cannot satisfy the adiabatic condition at the lateral surfaces. Therefore, this approach of isolating each contact region with a prism will not be considered in this paper. Instead, we will derive the expression for the constriction resistance by examining the thermal interactions of the contact regions. The approach used here is an extension of a powerful method first applied by Beck [5] to treat the problem of a square array of disks heated by a uniform flux. Beck's method has one advantage that for a given type of array, we need to calculate a number of lattice sums only once since they are readily applicable to different cases of disk boundary condition. Furthermore, for a given disk boundary condition, the solution techniques for different array types are essentially the same.

2. CASE 1: UNIFORM FLUX

We begin the analysis of a periodic array of identical disks heated by a uniform flux q_0 with that of a single disk on the surface of a semi-infinite solid. By separation of variables, the steady-state temperature in the solid is obtained as

$$T(\rho, z) = \frac{q_0 R}{k}\int_0^\infty \frac{1}{\tau} J_1(\tau) J_0(\tau\rho/R)\, e^{-\tau z/R}\, d\tau \quad (2)$$

where J_0 and J_1 are the Bessel function of the first kind of order zero and one, respectively. The cylindrical coordinate system (ρ, ϕ, z) has its origin at the center of the disk with the solid being described by $0 \leqslant \rho < \infty$, $0 \leqslant z < \infty$. The temperature T given by (2) vanishes as $z \to \infty$. At the solid surface, there is a uniform heat flux q_0 crossing the disk into the solid while the region external to the disk is insulated. From equation (2), we obtain the surface temperature as

$$T(\rho, z=0) = \frac{q_0 R}{k}\int_0^\infty \frac{1}{\tau} J_1(\tau) J_0(\tau\rho/R)\, d\tau. \quad (3)$$

Averaging (3) over the disk yields

$$\bar{T}(\rho < R, z=0) = \frac{8}{3\pi}\frac{q_0 R}{k}. \quad (4)$$

The temperature distribution of the solid surface outside the disk will be needed in the analysis later. Using a table of integrals [15], we expand the right hand side of (3) and obtain

$$T(\rho > R, z=0) = \frac{q_0 R}{k}\left[\frac{1}{2}\left(\frac{R}{\rho}\right) + \frac{1}{16}\left(\frac{R}{\rho}\right)^3 + \frac{3}{128}\left(\frac{R}{\rho}\right)^5 + \frac{25}{2048}\left(\frac{R}{\rho}\right)^7 + \frac{245}{32\,768}\left(\frac{R}{\rho}\right)^9 + \cdots\right]. \quad (5)$$

Next, we consider two disks of radius R on the surface of the solid as shown in Fig. 1. Let each of the disks be heated by a uniform flux q_0. Then, the temperature distribution T_{AB} over disk A contributed by disk B is equal to the right hand side of equation (5). To calculate the average of T_{AB} over disk A, $\bar{T}_{AB}$, we first expand T_{AB} in terms of the cylindrical polar coordinates (r, θ). This expansion can be accomplished by utilizing the Legendre polynomial identity

$$\left(\frac{R}{\rho}\right) = \left(\frac{R}{b}\right)\sum_{n=0}^{\infty}\left(\frac{r}{b}\right)^n P_n(\cos\theta) \quad (6)$$

and its derivatives

$$\left(\frac{R}{\rho}\right)^l = \frac{1}{1\cdot 3\cdots(l-2)}\left(\frac{R}{b}\right)^l \sum_{n=(l-1)/2}^{\infty}\left(\frac{r}{b}\right)^{n-(l-1)/2} \left.\frac{d^{(l-1)/2}P_n(x)}{dx^{(l-1)/2}}\right|_{x=\cos\theta} \quad (7)$$

where $l = 3, 5, 7, \ldots$. After a lot of algebra, we obtain

$$\bar{T}_{AB} = \frac{q_0 R}{k}\left[\frac{1}{2}\left(\frac{R}{b}\right) + \frac{1}{8}\left(\frac{R}{b}\right)^3 + \frac{15}{128}\left(\frac{R}{b}\right)^5 + \frac{175}{1024}\left(\frac{R}{b}\right)^7 + \frac{5145}{16\,384}\left(\frac{R}{b}\right)^9 + O\left\{\left(\frac{R}{b}\right)^{11}\right\}\right]. \quad (8)$$

2.1. *Square array of disks*

Having completed the analysis for two disks, we can now proceed to analyze the case of an infinite square array of disks. To do this, we first consider a square of sides $(2N+1)\delta$ on the surface of a semi-infinite solid and the $(2N+1)^2$ identical disks inside the square (Fig. 2), N being a large positive integer. The surface is insulated, except at the disks, each of which is heated by a uniform flux q_0. The disk at the center of the square, A, will be termed the reference disk. Later, the limit of $N \to \infty$ will be taken, thus recovering the infinite square array of disks.

Summing the right hand side of equation (8) over each of the disks inside the square, A being excluded, and combining the result with (4), we obtain the average temperature of the reference disk as

$$\bar{T}_A = \frac{q_0 R}{k}\left[\frac{8}{3\pi} + \frac{1}{2}s_1(N)\left(\frac{R}{\delta}\right) + \frac{1}{8}s_3(N)\left(\frac{R}{\delta}\right)^3 + \frac{15}{128}s_5(N)\left(\frac{R}{\delta}\right)^5 + \frac{175}{1024}s_7(N)\left(\frac{R}{\delta}\right)^7 + \frac{5145}{16\,384}s_9(N)\left(\frac{R}{\delta}\right)^9 + O\left\{\left(\frac{R}{\delta}\right)^{11}\right\}\right] \quad (9)$$

where

$$s_i(N) = (4 + 2^{(4-i)/2})\sum_{n=1}^{N}\frac{1}{n^i} + 8\sum_{n=1}^{N-1}\sum_{m=n+1}^{N}\frac{1}{(m^2+n^2)^{i/2}}. \quad (10)$$

The single sum in (10) corresponds to the summation

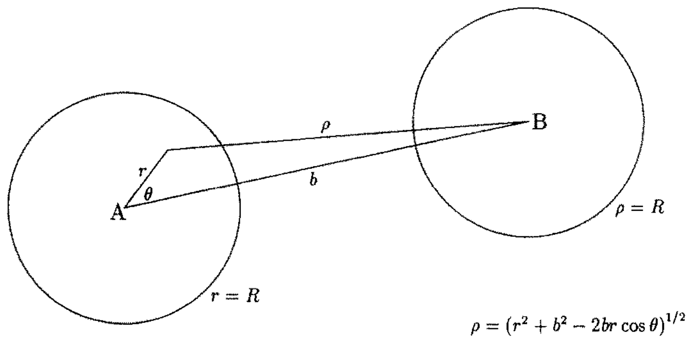

FIG. 1. Two circular disks of radius R on the surface of a semi-infinite solid.

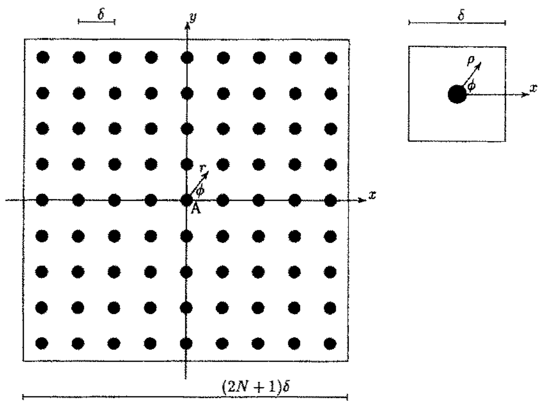

FIG. 2. Circular disks of radius R arranged in a square array on the surface of a semi-infinite solid. The disk at the center, labeled A, is the reference disk. Also shown are a typical disk and the unit cell associated with it.

over all the disks on the axes and the diagonals of the square, excluding the reference disk, while the double sums represent those located off the axes or diagonals. As $N \to \infty$, $s_1(N)$ becomes unbounded, indicating that with an infinite number of disks (heat sources) on the surface, the conditions of finite surface and zero far-field temperatures are incompatible with each other. Effectively, there is a uniform heat flux in the solid far away from its surface. Beck [5] handled this problem by introducing time dependence into his analysis. However, this is not necessary if we tolerate temperatures being finite at the solid surface while going linearly to infinity in the far field, which is a fairly common practice.

To overcome the difficulty of infinite average temperature of the reference disk, we take the difference between this average temperature and that of the entire solid surface. To calculate this temperature difference, we first suppose that the region of the surface inside the square was heated by the uniform flux $\tilde{q}$ given by

$$\tilde{q} = \frac{\pi R^2 q_0}{\delta^2} \tag{11}$$

the far-field temperature of the solid being zero. Then, the temperature at the center of the square would be [16]

$$\begin{aligned}\tilde{T} &= \frac{2}{\pi}\frac{\delta\tilde{q}}{k}(2N+1)\ln\tan\frac{3\pi}{8} \\ &= 2\frac{q_0 R}{k}\left(\frac{R}{\delta}\right)(2N+1)\ln\tan\frac{3\pi}{8}.\end{aligned} \tag{12}$$

Let

$$\Delta T \equiv \bar{T}_A - \tilde{T}. \tag{13}$$

Then, substituting (9) and (12) into (13), and letting $N \to \infty$, we obtain

$$\begin{aligned}\Delta T = \frac{q_0 R}{k}\Bigg[&\frac{8}{3\pi} + \frac{1}{2}S_1\left(\frac{R}{\delta}\right) + \frac{1}{8}S_3\left(\frac{R}{\delta}\right)^3 + \frac{15}{128}S_5\left(\frac{R}{\delta}\right)^5 \\ &+ \frac{175}{1024}S_7\left(\frac{R}{\delta}\right)^7 + \frac{5145}{16384}S_9\left(\frac{R}{\delta}\right)^9 + O\left\{\left(\frac{R}{\delta}\right)^{11}\right\}\Bigg]\end{aligned} \tag{14}$$

where

$$S_1 = \lim_{N\to\infty}\left[s_1(N) - (8N+4)\ln\tan\frac{3\pi}{8}\right] \tag{15}$$

$$S_i = \lim_{N\to\infty} s_i(N), \quad i = 3, 5, \ldots. \tag{16}$$

By numerical evaluation, it is found that S_1 is finite and is given by $S_1 = -3.90026$; the remaining sums are also evaluated numerically: $S_3 = 9.03362$, $S_5 = 5.09026$, $S_7 = 4.42312$, $S_9 = 4.19127$. Thus, ΔT given by (14) is finite.

With $N \to \infty$, we have thus recovered an infinite number of disks arranged in a square array. Furthermore, ΔT given by (14) becomes the difference between the average temperature of *any* disk and that of the entire solid surface. Substituting the rate of heat flow across a disk, $Q = \pi R^2 q_0$, and ΔT into (1), we obtain the dimensionless resistance as

$$\psi_s^{uf} = \frac{32}{3\pi^2} + \frac{2}{\pi} S_1^* \kappa^{1/2} + \frac{1}{2\pi} S_3^* \kappa^{3/2} + \frac{15}{32\pi} S_5^* \kappa^{5/2} + \frac{175}{256\pi} S_7^* \kappa^{7/2} + \frac{5145}{4096\pi} S_9^* \kappa^{9/2} + O(\kappa^{11/2}) \quad (17)$$

where

$$S_i^* = \frac{S_i}{\pi^{i/2}} \quad (18)$$

and $\kappa = \pi R^2/\delta^2$ is the area fraction of the solid surface occupied by the disks. Substituting the numerical values of the various S_i into (17) then yields

$$\psi_s^{uf} = 1.08076 - 1.4009\kappa^{1/2} + 0.25820\kappa^{3/2} + 0.043417\kappa^{5/2} + 0.017513\kappa^{7/2} + 0.0097061\kappa^{9/2} + O(\kappa^{11/2}). \quad (19)$$

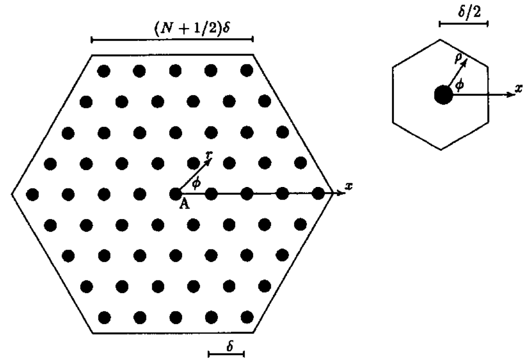

FIG. 3. Circular disks of radius R arranged in a hexagonal array on the surface of a semi-infinite solid. The disk at the center of the hexagon, labeled A, is the reference disk. A typical disk and its associated unit cell are also shown.

2.2. *Hexagonal array of disks*

For an infinite hexagonal array of disks on the surface of a semi-infinite solid, the analysis is similar to that for a square array. Consider first a large hexagon of sides $(N+1/2)\delta$ on the surface and the $[3N(N+1)+1]$ identical disks of radius R inside the hexagon, as shown in Fig. 3. The surface, except at the disks, is insulated. The disk at the center of the hexagon, A, is the reference disk. Later, we will take the limit of $N \to \infty$ to recover the infinite hexagonal array.

With each of the disks inside the hexagon heated by a uniform flux q_0, the average temperature of the reference disk is given by

$$\bar{T}_A = \frac{q_0 R}{k}\left[\frac{8}{3\pi} + \frac{1}{2}h_1(N)\left(\frac{R}{\delta}\right) + \frac{1}{8}h_3(N)\left(\frac{R}{\delta}\right)^3 + \frac{15}{128}h_5(N)\left(\frac{R}{\delta}\right)^5 + \frac{175}{1024}h_7(N)\left(\frac{R}{\delta}\right)^7 + \frac{5145}{16\,384}h_9(N)\left(\frac{R}{\delta}\right)^9 + O\left\{\left(\frac{R}{\delta}\right)^{11}\right\}\right] \quad (20)$$

where

$$h_i(N) = 6\sum_{n=1}^{N}\frac{1}{n^i} + 6\sum_{n=1}^{N-1}\sum_{m=n+1}^{N}\frac{1}{(m^2-mn+n^2)^{i/2}}. \quad (21)$$

The single sum in (21) corresponds to the summation of (8) over all the disks located on the diagonals of the hexagon, the reference disk being excluded, while the double sums represent those located off the diagonals. Like $s_1(N)$, $h_1(N)$ becomes infinite as $N \to \infty$, and the problem of infinite $\bar{T}_A$ can be taken care of in a way similar to that of a square array.

Thus, following the same procedure employed in the analysis of a square array, we obtain the constriction resistance for an infinite hexagonal array of disks as

$$\psi_h^{uf} = \frac{32}{3\pi^2} + \frac{2}{\pi} H_1^* \kappa^{1/2} + \frac{1}{2\pi} H_3^* \kappa^{3/2} + \frac{15}{32\pi} H_5^* \kappa^{5/2} + \frac{175}{256\pi} H_7^* \kappa^{7/2} + \frac{5145}{4096\pi} H_9^* \kappa^{9/2} + O(\kappa^{11/2}) \quad (22)$$

where

$$H_i^* = \left(\frac{\sqrt{3}}{2}\right)^{i/2} \frac{H_i}{\pi^{i/2}} \quad (23)$$

$$H_1 = \lim_{N\to\infty}[h_1(N) - (6N+3)\ln 3] \quad (24)$$

$$H_i = \lim_{N\to\infty} h_i(N), \quad i = 3, 5, \ldots \quad (25)$$

and $\kappa = 2\pi R^2/\delta^2\sqrt{3}$ is the area fraction of the disks. Then, substituting the numerical values of $H_1 = -4.21342$, $H_3 = 11.0342$, $H_5 = 6.76190$, $H_7 = 6.19524$, and $H_9 = 6.05695$ into (22) results in

$$\psi_h^{uf} = 1.08076 - 1.4083\kappa^{1/2} + 0.25417\kappa^{3/2} + 0.040254\kappa^{5/2} + 0.014827\kappa^{7/2} + 0.0073425\kappa^{9/2} + O(\kappa^{11/2}). \quad (26)$$

2.3. *Triangular array of disks*

The analysis for an infinite triangular array of disks on the surface of a semi-infinite solid is similar to the previous ones. First, we consider a large equilateral triangle of sides $\sqrt{3}(3N+1)\delta$ on the surface and the $(9N^2+6N+1)$ identical disks of radius R inside the triangle, as shown in Fig. 4. The surface, except at the disks, is insulated. The disk at the center of the hexagon, A, is the reference disk. Both the large triangle and the unit cell associated with the reference disk have the same orientation. To recover the infinite triangular array, we take the limit of $N \to \infty$.

With a uniform flux of q_0 applied to each of the disks inside the triangle, the average temperature of the reference disk takes the form

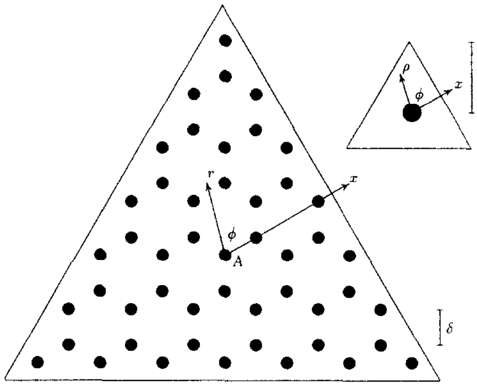

FIG. 4. Circular disks of radius R arranged in a triangular array on the surface of a semi-infinite solid. The reference disk, A, is located at the center of the triangle. Also shown are a typical disk and its associated unit cell.

$$\bar{T}_A = \frac{q_0 R}{k}\left[\frac{8}{3\pi}+\frac{1}{2}t_1(N)\left(\frac{R}{\delta}\right)+\frac{1}{8}t_3(N)\left(\frac{R}{\delta}\right)^3 + \frac{15}{128}t_5(N)\left(\frac{R}{\delta}\right)^5+\frac{175}{1024}t_7(N)\left(\frac{R}{\delta}\right)^7 + \frac{5145}{16384}t_9(N)\left(\frac{R}{\delta}\right)^9+O\left\{\left(\frac{R}{\delta}\right)^{11}\right\}\right] \quad (27)$$

where

$$t_i(N) = 3\sum_{n=1}^{N}\left\{\frac{1}{(3n-1)^i}+\frac{1}{(3n)^i}\right\} + 3\sum_{n=1}^{N}\left\{\sum_{m=1}^{3n-2}\frac{1}{[(3n-1)^2+3m^2-3m(3n-1)]^{i/2}} + \sum_{m=1}^{3n-1}\frac{1}{[9n^2+3m^2-9mn]^{i/2}}\right\}. \quad (28)$$

The single sum in (28) corresponds to summing equation (8) over each of the disks located on the segments joining the center and the vertices of the triangle, while the double sums correspond to the summation over the disks located off these segments. Again, $t_1(N)$ becomes unbounded when $N \to \infty$.

After a little bit of algebra, we obtain the constriction resistance for an infinite triangular array of disks as

$$\psi_t^{uf} = \frac{32}{3\pi^2}+\frac{2}{\pi}T_1^*\kappa^{1/2}+\frac{1}{2\pi}T_3^*\kappa^{3/2}+\frac{15}{32\pi}T_5^*\kappa^{5/2} + \frac{175}{256\pi}T_7^*\kappa^{7/2}+\frac{5145}{4096\pi}T_9^*\kappa^{9/2}+O(\kappa^{11/2}) \quad (29)$$

where

$$T_i^* = \left(\frac{3\sqrt{3}}{4}\right)^{i/2}\frac{T_i}{\pi^{i/2}} \quad (30)$$

$$T_1 = \lim_{N\to\infty}\left[t_1(N)-\frac{4}{\sqrt{3}}(3N+1)\ln\tan\frac{5\pi}{12}\right] \quad (31)$$

$$T_i = \lim_{N\to\infty} t_i(N), \quad i = 3, 5, \ldots. \quad (32)$$

Here, the area fraction of the solid surface occupied by the disks is given by $\kappa = 4\pi R^2/3\delta^2\sqrt{3}$. Substituting the numerical values of $T_1 = -3.32302$, $T_3 = 6.57885$, $T_5 = 3.59784$, $T_7 = 3.16386$, and $T_9 = 3.05006$ into (29) then yields

$$\psi_t^{uf} = 1.08076-1.3603\kappa^{1/2}+0.27841\kappa^{3/2} + 0.059022\kappa^{5/2}+0.031298\kappa^{7/2} + 0.022925\kappa^{9/2}+O(\kappa^{11/2}). \quad (33)$$

3. CASE 2: EQUIVALENT ISOTHERMAL FLUX

Consider a semi-infinite solid heated by the equivalent isothermal flux

$$q_E = q_0\left[1-\left(\frac{\rho}{R}\right)^2\right]^{-1/2} \quad (34)$$

over a circular region of radius R on the surface, the region external to the disk being insulated. Then, with the far-field temperature of the solid held at zero, the steady-state surface temperature is given by

$$T(\rho, z=0) = \begin{cases} \dfrac{\pi}{2}\dfrac{q_0 R}{k} & \text{if } \rho < R \\ \dfrac{q_0 R}{k}\sin^{-1}\left(\dfrac{R}{\rho}\right) & \text{if } \rho > R. \end{cases} \quad (35)$$

From (35), it is seen that the equivalent isothermal flux can be used to replace the condition of uniform temperature of an array of isothermal disks, provided the disks are sufficiently far apart. In fact, q_E is the leading-order heat flux in the analysis of an array of isothermal disks; we will discuss this in greater detail in the next section. Expanding the factor of $\sin^{-1}(R/\rho)$ in equation (35), we obtain

$$T(\rho > R, z=0) = \frac{q_0 R}{k}\left[\left(\frac{R}{\rho}\right)+\frac{1}{6}\left(\frac{R}{\rho}\right)^3 + \frac{3}{40}\left(\frac{R}{\rho}\right)^5+\frac{5}{112}\left(\frac{R}{\rho}\right)^7+\frac{35}{1152}\left(\frac{R}{\rho}\right)^9+\cdots\right]. \quad (36)$$

Equation (36) is the counterpart of (5). Thus, following the same procedure employed in the last section, we obtain the constriction resistance for an infinite square array of disks as

$$\psi_s^{eif} = 1+\frac{2}{\pi}S_1^*\kappa^{1/2}+\frac{7}{12\pi}S_3^*\kappa^{3/2}+\frac{99}{160\pi}S_5^*\kappa^{5/2} + \frac{3575}{3584\pi}S_7^*\kappa^{7/2}+\frac{146965}{73728\pi}S_9^*\kappa^{9/2}+O(\kappa^{11/2}) \quad (37)$$

$$= 1-1.4009\kappa^{1/2}+0.30123\kappa^{3/2}+0.057310\kappa^{5/2} + 0.025554\kappa^{7/2}+0.015403\kappa^{9/2}+O(\kappa^{11/2}). \quad (38)$$

For a hexagonal array of disks, the resistance is given by

$$\psi_h^{\text{cif}} = 1+\frac{2}{\pi}H_1^*\kappa^{1/2}+\frac{7}{12\pi}H_3^*\kappa^{3/2}+\frac{99}{160\pi}H_5^*\kappa^{5/2}$$

$$+\frac{3575}{3584\pi}H_7^*\kappa^{7/2}+\frac{146\,965}{73\,728\pi}H_9^*\kappa^{9/2}+O(\kappa^{11/2}) \quad (39)$$

$$= 1-1.4083\kappa^{1/2}+0.29654\kappa^{3/2}+0.053136\kappa^{5/2}$$

$$+0.021635\kappa^{7/2}+0.011652\kappa^{9/2}+O(\kappa^{11/2}) \quad (40)$$

and for a triangular array

$$\psi_t^{\text{cif}} = 1+\frac{2}{\pi}T_1^*\kappa^{1/2}+\frac{7}{12\pi}T_3^*\kappa^{3/2}+\frac{99}{160\pi}T_5^*\kappa^{5/2}$$

$$+\frac{3575}{3584\pi}T_7^*\kappa^{7/2}+\frac{146\,965}{73\,728\pi}T_9^*\kappa^{9/2}+O(\kappa^{11/2}) \quad (41)$$

$$= 1-1.3603\kappa^{1/2}+0.32481\kappa^{3/2}+0.077909\kappa^{5/2}$$

$$+0.045670\kappa^{7/2}+0.036380\kappa^{9/2}+O(\kappa^{11/2}). \quad (42)$$

4. CASE 3: ISOTHERMAL CONDITION

The problem of an array of isothermal disks on the otherwise insulated surface of a semi-infinite solid is very complicated due to the multiply connected mixed boundary conditions. However, Tio [17] has shown that the isothermal condition of the disks can be replaced with a series of heat fluxes. For a square array and a hexagonal array, the leading terms of the series are, respectively

$$q_s = q_0\Theta^{-1/2}$$

$$-\frac{q_0}{\pi}(\Theta^{-1/2}-2\Theta^{1/2})S_3^*\kappa^{3/2}$$

$$-\frac{q_0}{4\pi}(9\Theta^{-1/2}-24\Theta^{1/2}+8\Theta^{3/2})S_5^*\kappa^{5/2}$$

$$-\frac{4q_0}{\pi}\left(\frac{\rho}{R}\right)^4\Theta^{-1/2}\cos 4\phi S_{5,4}^*\kappa^{5/2}$$

$$+\frac{q_0}{3\pi^2}(\Theta^{-1/2}-2\Theta^{1/2})S_3^*S_3^*\kappa^{6/2}$$

$$-\frac{q_0}{24\pi}(135\Theta^{-1/2}-480\Theta^{1/2}$$

$$+320\Theta^{3/2}-48\Theta^{5/2})S_7^*\kappa^{7/2}$$

$$-\frac{4q_0}{\pi}\left(\frac{\rho}{R}\right)^4(2\Theta^{-1/2}-\Theta^{1/2})\cos 4\phi S_{7,4}^*\kappa^{7/2}$$

$$+O(\kappa^{8/2}) \quad (43)$$

and

$$q_h = q_0\Theta^{-1/2}$$

$$-\frac{q_0}{\pi}(\Theta^{-1/2}-2\Theta^{1/2})H_3^*\kappa^{3/2}$$

$$-\frac{q_0}{4\pi}(9\Theta^{-1/2}-24\Theta^{1/2}+8\Theta^{3/2})H_5^*\kappa^{5/2}$$

$$+\frac{q_0}{3\pi^2}(\Theta^{-1/2}-2\Theta^{1/2})H_3^*H_3^*\kappa^{6/2}$$

$$-\frac{q_0}{24\pi}(135\Theta^{-1/2}-480\Theta^{1/2}$$

$$+320\Theta^{3/2}-48\Theta^{5/2})H_7^*\kappa^{7/2}$$

$$-\frac{4q_0}{\pi}\left(\frac{\rho}{R}\right)^6\Theta^{-1/2}\cos 6\phi H_{7,6}^*\kappa^{7/2}$$

$$+O(\kappa^{8/2}) \quad (44)$$

where

$$\Theta = 1-\left(\frac{\rho}{R}\right)^2 \quad (45)$$

$$S_{i,4}^* = \frac{1}{\pi^{i/2}}\lim_{N\to\infty} s_{i,4}(N) \quad (46)$$

$$s_{i,4}(N) = (4-2^{(4-i)/2})\sum_{n=1}^{N}\frac{1}{n^i}$$

$$+8\sum_{n=1}^{N-1}\sum_{m=n+1}^{N}\frac{1}{(m^2+n^2)^{i/2}}\left[2\left(\frac{m^2-n^2}{m^2+n^2}\right)^2-1\right] \quad (47)$$

$$H_{i,6}^* = \left(\frac{\sqrt{3}}{2}\right)^{i/2}\frac{1}{\pi^{i/2}}\lim_{N\to\infty} h_{i,6}(N) \quad (48)$$

$$h_{i,6}(N) = 6\sum_{n=1}^{N}\frac{1}{n^i}$$

$$+6\sum_{n=1}^{N-1}\sum_{m=n+1}^{N}\frac{1}{(m^2-mn+n^2)^{i/2}}$$

$$\times\left[1-\frac{27}{2}\frac{m^2n^2(m-n)^2}{(m^2-mn+n^2)^3}\right]. \quad (49)$$

The coordinate system (ρ, ϕ) has its origin at the center of the disk to which q_s or q_h is applied. The orientation of the coordinate axes is shown in Figs. 2 and 3. Application of q_s or q_h as given above to each of the disks in the respective array results in disk temperature uniform up to $O(\kappa^{7/2})$. In both (43) and (44), the leading-order term is simply the equivalent isothermal flux, which has been shown [17] to approximate the isothermal condition with non-uniformity in disk temperature occurring as early as $O(\kappa^{3/2})$.

Using the heat fluxes given above, and following the same procedure utilized in the previous sections, we can then derive the expressions for the constriction resistance. For a square array, the resistance is given by

$$\psi_s^{i} = 1+\frac{2}{\pi}S_1^*\kappa^{1/2}+\frac{3}{3\pi}S_3^*\kappa^{3/2}+\frac{4}{5\pi}S_5^*\kappa^{5/2}$$

$$-\frac{4}{45\pi^2}S_3^*S_3^*\kappa^{6/2}+\frac{10}{7\pi}S_7^*\kappa^{7/2}+\cdots \quad (50)$$

$$= 1-1.4009\kappa^{1/2}+0.34427\kappa^{3/2}+0.074098\kappa^{5/2}$$

$$-0.023704\kappa^{6/2}+0.036598\kappa^{7/2}+\cdots \quad (51)$$

while the resistance of a hexagonal array is

$$\psi_{\mathrm{h}}^{\mathrm{i}} = 1+\frac{2}{\pi}H_1^*\kappa^{1/2}+\frac{2}{3\pi}H_3^*\kappa^{3/2}+\frac{4}{5\pi}H_5^*\kappa^{5/2}$$

$$-\frac{4}{45\pi^2}H_3^*H_3^*\kappa^{6/2}+\frac{10}{7\pi}H_7^*\kappa^{7/2}+\cdots \quad (52)$$

$$= 1-1.4083\kappa^{1/2}+0.33890\kappa^{3/2}+0.068701\kappa^{5/2}$$

$$-0.022971\kappa^{6/2}+0.030984\kappa^{7/2}+\cdots. \quad (53)$$

It should be noted that (50) and (52) consist of the first six terms of the complete expansion of the exact resistance for the case of truly isothermal disks. Therefore, ψ as given by (50) and (52) corresponds to disks uniform in temperature up to $O(\kappa^{7/2})$. In principle, the approximation can be improved by carrying additional terms (of higher order) in (50) and (52), the new expressions corresponding to an even higher order of uniformity in disk temperature. However, the heat fluxes as given in (43) and (44) will be inadequate, since the contributions from the fluxes of $O(\kappa^{8/2})$ and higher must then be included in (50) and (52).

5. DISCUSSION

We have derived analytical expressions of the constriction resistance for different disk boundary conditions and disk arrangements. In these expressions, the leading term depends only on the disk boundary condition while its first-order perturbation is a function of disk arrangement only (for a given type of array and any one of the three disk boundary conditions considered here, the coefficients of $\kappa^{1/2}$ are identical). However, perturbations of higher order ($\kappa^{i/2}$, $i \geqslant 3$) are functions of both the disk boundary condition and arrangement. Nevertheless, each term can be considered as a product of two factors, each of which depends on either the disk boundary condition or disk arrangement only.

Since the expressions for the constriction resistance involve an infinite series, we need to check if the number of terms we have obtained for each series is sufficient to give accurate results. For $\kappa = 0.6$, which corresponds to the case of nearly touching neighboring disks in a triangular array, it can be seen from equation (33) that the contribution from the $O(\kappa^{11/2})$ term is less than 0.8% of the resistance calculated using the first six terms of the series. For (42), (19), (38), (26) and (40), the corresponding figures are 1.7, 0.5, 1.3, 0.4, and 1.1%, respectively. Thus, for $\kappa \leqslant 0.6$, the six formulas are adequate. In fact, we can even go up to $\kappa = 0.7$ for a square array or a hexagonal array of disks with uniform flux; in this case, the contribution from the $O(\kappa^{11/2})$ term is less than 1.7 and 1.5% for a square array and a hexagonal array, respectively.

While each term of $O(\kappa^{3/2})$ or higher in the series in the resistance formulas is positive for cases of uniform flux and equivalent isothermal flux, the resistance formulas for isothermal disks, equations (51) and (53), consist of positive and negative terms. Therefore, we can expect that they converge faster. At $\kappa = 0.6$, the difference between using the first four terms and the first six terms of (51) is less than 1.1%; for (53), the difference is less than 0.3%. At $\kappa = 0.7$, the corresponding figures are 3.9 and 2.1%. Thus, for practical purposes, formulas (51) and (53) are adequate.

The constriction resistance of a square array of disks has been calculated by a few investigators. For disks heated by a uniform flux or the equivalent isothermal flux, Negus and Yovanovich [12] obtained numerical correlations which, adjusted to the notation of the present study, take the forms of

$$\psi_{\mathrm{s}}^{\mathrm{uf}} = 1.08076-1.40043\kappa^{1/2}+0.26162\kappa^{3/2}$$

$$+0.0151\kappa^{5/2}+0.090639\kappa^{7/2} \quad (54)$$

$$\psi_{\mathrm{s}}^{\mathrm{eif}} = 1.00000-1.40079\kappa^{1/2}+0.30153\kappa^{3/2}$$

$$+0.04966\kappa^{5/2}+0.06447\kappa^{7/2}. \quad (55)$$

For $\kappa \leqslant 0.6$, equations (54) and (55) agree with the respective formulas derived in this study, which predict lower values of resistance, to within 3.9%. An analytical expression for the case of uniform flux was derived by Beck [5]

$$\psi_{\mathrm{s}}^{\mathrm{uf}} = 1.080759-1.40087\kappa^{1/2}+0.12910\kappa^{3/2}. \quad (56)$$

While the coefficient of $\kappa^{3/2}$ in (56) is only half of that in (19), a formal treatment to $O(\kappa^{3/2})$ would yield the latter result. As stated before, the expressions for the resistance were also derived by Sadhal [13] for cases of uniform flux and the equivalent isothermal flux for the square prism. The solution for the uniform flux case was later used by Negus *et al.* [14]. These expressions, however, involve infinite double series of Bessel functions and are more complicated than the formulas derived in this study. For $\kappa^{1/2} = 0.1, 0.2, 0.3, 0.4$ and 0.5, the values of $\psi_{\mathrm{s}}^{\mathrm{uf}}$ and $\psi_{\mathrm{s}}^{\mathrm{eif}}$ were evaluated to four-digit accuracy, and agree exactly with the respective formulas derived in this paper. It seems that no other works of a hexagonal or a triangular array of disks exist in the literature, although an investigation of a multiply connected contact region with a hexagonal array of circular gaps (regions of no contact) has been carried out [18]. In what follows, the results are those obtained in this study, unless stated otherwise.

Figure 5 shows the resistance of a hexagonal array of disks for three cases of disk boundary condition: uniform flux, uniform temperature, and the equivalent isothermal flux. For a square array, the same feature is also observed, i.e. the resistance of isothermal disks is smaller than that of disks with uniform flux but is larger than that of disks heated by the equivalent isothermal flux. From Fig. 5, we see that the uniform-flux condition is not a good approximation to the disk boundary condition of uniform temperature. While the equivalent isothermal flux and the isothermal condition predict nearly the same resistance for small κ, the relative difference can be

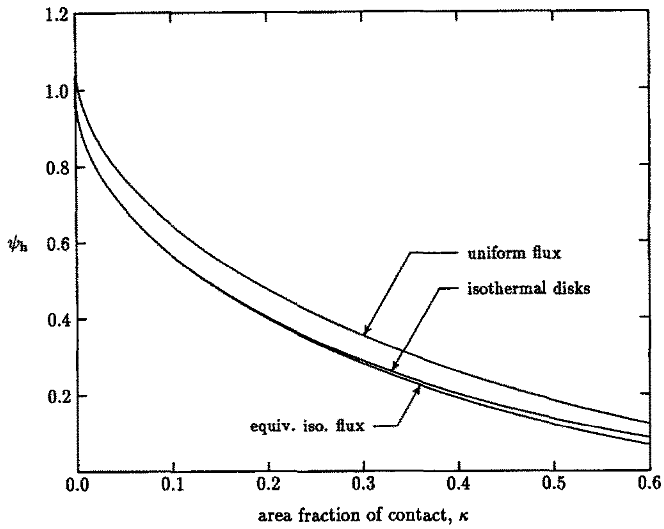

FIG. 5. Resistance ψ_h of a hexagonal array of disks for three cases of boundary condition—uniform flux, uniform temperature, and equivalent isothermal flux.

quite significant when κ increases. In particular, at $\kappa = 0.6$, the quantity $(\psi_h^i - \psi_h^{eif})/\psi_h^i$ is about 23% ; for a square array at $\kappa = 0.6$, $(\psi_s^i - \psi_s^{eif})/\psi_s^i$ is about 21%. Thus, the choice of boundary conditions plays a very important role in the prediction of the constriction resistance, especially when the area fraction of contact is large.

It is interesting to see how the arrangement of disks affects the constriction resistance. In Fig. 6, we plot the resistance ψ of disks with uniform flux for the three types of array considered in this study. As expected, the resistance decreases as the unit cells of the array change from a triangle to a square, and to a hexagon, κ being kept constant. In other words, the closer the unit cells come to full lateral isotropy (circular cell), the lower the resistance will be. This point is confirmed by the fact that the resistance for a disk on a laterally insulated semi-infinite cylinder assumes the smallest values. Furthermore, compared to the correlation for the cylindrical resistance obtained by Negus and Yovanovich [12]

$$\psi_c^{uf} = 1.08076 - 1.41042\kappa^{1/2} + 0.26604\kappa^{3/2} - 0.00016\kappa^{5/2} + 0.058266\kappa^{7/2} \quad (57)$$

the hexagonal resistance never exceeds the cylindrical resistance by more than 1% over the range of $0 \leqslant \kappa \leqslant 0.6$. In Fig. 7, we plot the fraction by which the resistance increases

$$\Omega \equiv \frac{\psi - \psi_h}{\psi_h} \quad (58)$$

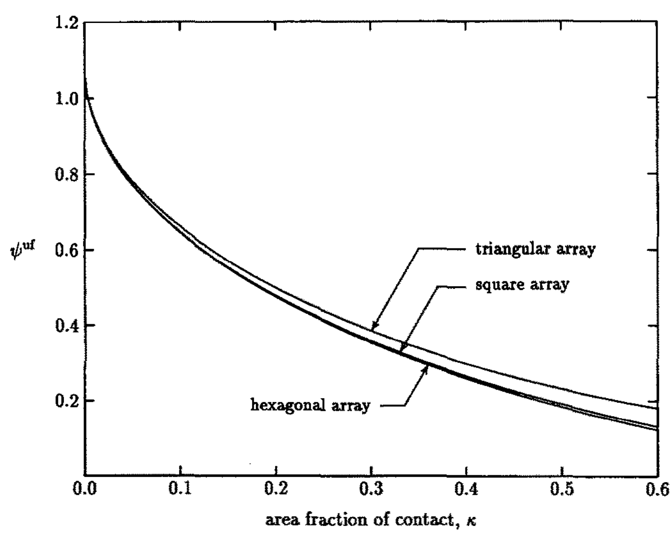

FIG. 6. Resistance ψ^{uf} for three different arrays of disks heated by a uniform flux.

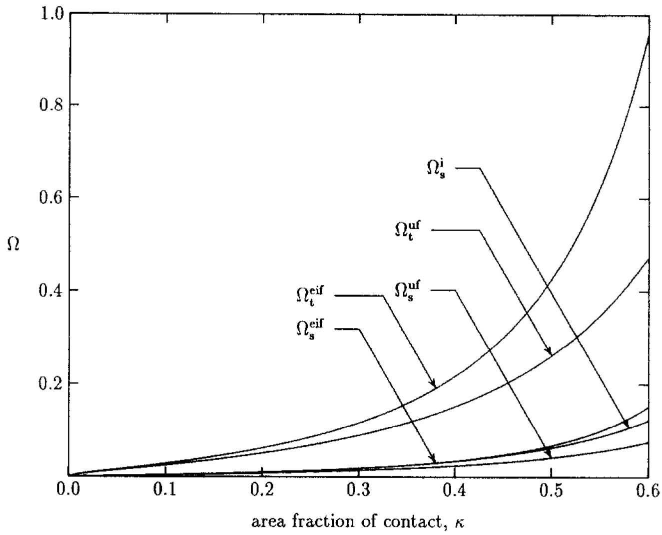

Fig. 7. Fractional increase in resistance, Ω, for a square array and a triangular array of disks for various cases of boundary condition.

when the array type changes from a hexagon to a square or a triangle. While the resistance formula for a triangular array of isothermal disks is not available, we can expect that $\Omega_t^i > \Omega_s^i$ for $\kappa \neq 0$. Furthermore, we can also anticipate that $\Omega_t^{uf} < \Omega_t^i < \Omega_t^{eif}$. From Fig. 7, we see that for small κ, the effects of disk arrangement on the constriction resistance are negligible; however, they become significant when κ increases. In particular, we see that at $\kappa = 0.6$, $\Omega_s^i \simeq 12\%$ while Ω_t^i may be as high as 60%.

As mentioned earlier, the temperature of the contact regions is uniform. To keep the problem tractable while at the same time reflecting this isothermal condition, the cylindrical cell model, which consists of an isothermal disk on top of a laterally insulated coaxial semi-infinite cylinder, has been widely used. Thus, it will be interesting to compare the cylindrical cell model to the periodic arrays considered in this study. To this end, we make use of the correlation obtained by Negus and Yovanovich [8, 12]

$$\psi_c^i = 1 - 1.40978\kappa^{1/2} + 0.34406\kappa^{3/2} + 0.04305\kappa^{5/2} + 0.02271\kappa^{7/2} \quad (59)$$

and plot the relative difference in resistance

$$\Lambda \equiv \frac{\psi^i - \psi_c^i}{\psi_c^i} \quad (60)$$

for a square array and a hexagonal array of (isothermal) disks in Fig. 8. For $0 \leqslant \kappa \leqslant 0.6$, Λ_h is less

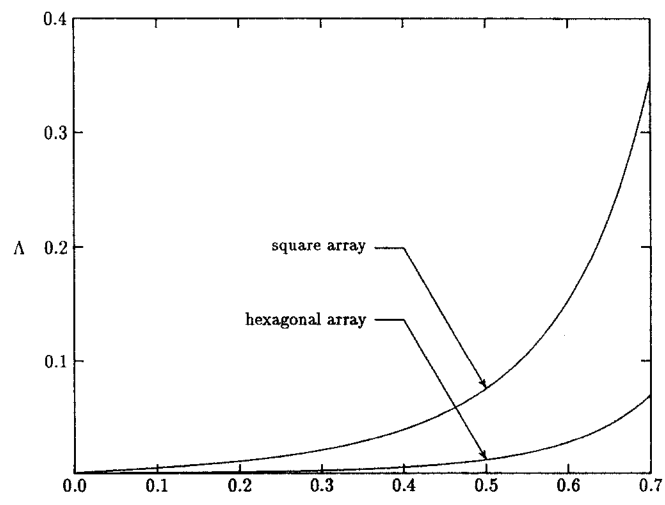

Fig. 8. Relative difference in resistance, Λ, between a square array or a hexagonal array and the cylindrical cell model.

than 3%, and for practical purposes, a hexagonal array and a cylindrical cell are interchangeable. Beyond $\kappa = 0.6$, however, Λ_h increases quite rapidly. In the case of a square array, we may incur significant errors if we model it with a cylindrical cell when $\kappa \geqslant 0.45$. For example, Λ_s may exceed 30% at $\kappa = 0.7$. These points are worth considering when one models multiple-contact problems with a single contact area on top of a circular cylinder.

6. CONCLUSION

We have demonstrated the importance of the boundary condition prescribed over the contact regions in the prediction of the constriction resistance. In general, the condition of uniform flux is not a good approximation to the boundary condition of isothermal contact regions. There may be circumstances, however, under which the physical representation calls for a uniform flux condition. While the equivalent isothermal flux predicts accurate results for small κ, the errors incurred may become significant when κ increases. We have also shown the effects of disk arrangement and concentration on the resistance. When the contact regions are far apart, the effects of disk arrangement are negligible. However, they become significant when κ increases. This is true whether we impose the isothermal boundary condition or prescribe the equivalent isothermal flux or uniform flux over the contact areas.

While the present model of periodic arrays of identical contact regions is somewhat specialized compared to the situation of contact regions of random sizes in random spatial distribution, it has nevertheless yielded valuable information. The random problem is exceedingly complicated, and analytical treatment of it is yet to be developed. Recently, Das and Sadhal [19] have taken up the first step towards that goal.

Acknowledgements—The authors are very grateful to the U.S. National Science Foundation for the support of this work under Grant Nos. CBT-8351432 and INT-8807482. Thanks are also due to D.A.M.T.P. (Cambridge University) for the availability of their research facilities to the second author (S.S.S.), who was on a sabbatical leave there (5 July 1988–18 July 1989).

REFERENCES

1. C. V. Madhusudana and L. S. Fletcher, Contact heat transfer—the last decade, *AIAA J.* **24,** 510–523 (1986).
2. M. M. Yovanovich, Recent developments in thermal contact, gap and joint conductance theories and experiment, *Proc. Eighth Int. Heat Transfer Conf.*, Vol. 1, pp. 35–45. Hemisphere, Washington, DC (1986).
3. L. S. Fletcher, Recent developments in contact conductance heat transfer, *J. Heat Transfer* **110,** 1059–1070 (1988).
4. H. S. Carslaw and J. C. Jaeger, *Conduction of Heat in Solids*, pp. 214–217. Oxford University Press, London (1959).
5. J. V. Beck, Effects of multiple sources in the contact conductance theory, *J. Heat Transfer* **101,** 132–136 (1979).
6. A. Hunter and A. Williams, Heat flow across metallic joints—the constriction alleviation factor, *Int. J. Heat Mass Transfer* **12,** 524–526 (1969).
7. R. D. Gibson, The contact resistance for a semi-infinite cylinder in a vacuum, *Appl. Energy* **2,** 57–65 (1976).
8. K. J. Negus and M. M. Yovanovich, Constriction resistance of circular flux tubes with mixed boundary conditions by linear superposition of Neumann solutions, ASME Paper 84-HT-84 (1984).
9. G. M. L. Gladwell and T. F. Lemczyk, Thermal constriction resistance of a contact on a circular cylinder with mixed convective boundaries, *Proc. R. Soc. Lond.* **A420,** 323–354 (1988).
10. K. J. Negus, M. M. Yovanovich and J. W. DeVaal, Development of thermal constriction resistance for anisotropic rough surfaces by the method of infinite images, ASME Paper 85-HT-17 (1985).
11. G. K. Batchelor, Sedimentation in a dilute dispersion of spheres, *J. Fluid Mech.* **52,** 245–268 (1972).
12. K. J. Negus and M. M. Yovanovich, Application of the method of optimized images to steady three-dimensional conduction problems, ASME Paper 84-WA/HT-110 (1984).
13. S. S. Sadhal, Exact solutions for the steady and unsteady diffusion problems for a rectangular prism: cases of complex Neumann conditions, ASME Paper 84-HT-83 (1984).
14. K. J. Negus, M. M. Yovanovich and J. V. Beck, On the nondimensionalization of constriction resistance for semi-infinite heat flux tubes, *J. Heat Transfer* **111,** 804–807 (1989).
15. I. S. Gradshteyn and I. M. Ryzhik, *Table of Integrals, Series, and Products*, p. 692. Academic Press, New York (1980).
16. M. M. Yovanovich, Thermal constriction resistance of contacts on a half-space: integral formulation. In *Progress in Astronautics and Aeronautics: Radiative Transfer and Thermal Control*, Vol. 49, pp. 397–418. AIAA, New York (1976).
17. K.-K. Tio, Transport problems with spatially periodic mixed interface conditions, Ph.D. Thesis, University of Southern California, Los Angeles (1990).
18. K.-K. Tio and S. S. Sadhal, Analysis of thermal constriction resistance with adiabatic circular gaps, *J. Thermophys. Heat Transfer* **5,** 550–559 (1991).
19. A. K. Das and S. S. Sadhal, The effect of clustering in thermal contact resistance, *Proc. Ninth Int. Heat Transfer Conf.*, Vol. 5, pp. 517–522. Hemisphere, New York (1990).

RESISTANCE THERMIQUE DE CONSTRICTION: EFFETS DES CONDITIONS AUX LIMITES ET DES GEOMETRIES DU CONTACT

Résumé—Le problème de la résistance thermique de constriction permanente est modélisé au moyen de plusieurs arrangements spatialement périodiques de disques circulaires (régions de contact) sur la surface d'un solide semi-infini. On considère trois cas de conditions aux limites du disque: flux uniforme, "flux isotherme équivalent" et disques isothermes. Des expériences analytiques pour la résistance sont données en série puissance de $\kappa^{1/2}$ où κ est la fraction de surface solide occupée par les disques. Le comportement de la résistance est ensuite étudiée en fonction de la condition aux limites du disque, de l'arrangement spatial et de la concentration.

EINFLUSS DER RANDBEDINGUNGEN UND DER KONTAKTGEOMETRIE AUF DEN THERMISCHEN KONTAKTWIDERSTAND

Zusammenfassung—Das Problem des stationären thermischen Kontaktwiderstands wird durch unterschiedliche räumlich periodische Anordnungen von Kreisscheiben (Kontaktgebieten) an der Oberfläche eines halbunendlichen Festkörpers dargestellt. Drei unterschiedliche Randbedingungen werden betrachtet: Gleichförmige Wärmestromdichte, "äquivalente isotherme Stromdichte" und der Fall isothermer Scheiben. Für den Widerstand ergeben sich analytische Ausdrücke in Form von Potenzreihen mit dem Argument $\kappa^{1/2}$, wobei κ den Anteil an der Festkörperoberfläche darstellt, der von den Scheiben eingenommen wird. Das Verhalten des Widerstands wird dann abhängig von den Randbedingungen an den Scheiben, von deren räumlicher Anordnung und Konzentration untersucht.

ТЕПЛОВОЕ СОПРОТИВЛЕНИЕ ПРИ СЖАТИИ: ЭФФЕКТЫ ГРАНИЧНЫХ УСЛОВИЙ И ГЕОМЕТРИИ УЧАСТКОВ КОНТАКТА

Аннотация—С помощью различных пространственно периодических распложений круглых дисков (участков контакта) на поверхности полуограниченного твердого тела моделируется задача стационарного теплового сопротивления при сжатии. Исследуются три случая граничных условий на дисках: однородный тепловой поток, "эквивалентный изотермический поток" и условие изотермичности дисков. Получены аналитические выражения для сопротивления в виде степенного ряда по $\kappa^{1/2}$, где κ-часть поверхности твердого тела, занятая дисками. Исследуется характер сопротивления в зависимости от граничных условий на дисках, их пространственного расположения и концентрации.